

**Charge Effects Regulate Reversible CO₂ Reduction Catalysis**

Journal:	<i>ChemComm</i>
Manuscript ID	CC-COM-05-2018-004370.R1
Article Type:	Communication

SCHOLARONE™
Manuscripts



ChemComm

COMMUNICATION

Charge Effects Regulate Reversible CO₂ Reduction Catalysis

Jacob B. Geri, Joanna L. Ciatti, and Nathaniel K. Szymczak *

Received 00th January 20xx,
Accepted 00th January 20xx

DOI: 10.1039/x0xx00000x

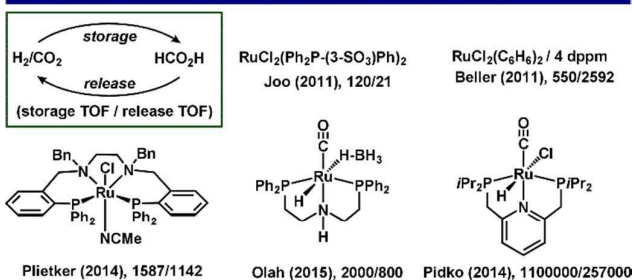
www.rsc.org/

Modular but geometrically constrained ligands were used to investigate the impact of key ligand design parameters (charge and bite angle) on CO₂ hydrogenation and formic acid dehydrogenation activity. These studies yielded an optimized catalyst that achieved over 118,000 turnovers in CO₂ hydrogenation, 247,000 turnovers in HCO₂H dehydrogenation, was applied in a hydrogen storage device used for 6 cycles of hydrogen storage/release without requiring changes in pH or solvent, and generated H₂/CO₂ gas at a pressure of 190 atm from formic acid.

Hydrogen represents a promising energy carrier¹ and features a high energy density by weight (120 MJ kg⁻¹), yet low volumetric energy density (0.0108 MJ L⁻¹). The latter attribute precludes the use of gaseous hydrogen, and is a major liability that can be overcome with liquid carriers (needed for transport/delivery) that contain covalently bound hydrogen.² One highly studied low molecular weight carrier is formic acid (HCO₂H): a non-volatile biodegradable liquid at room temperature that can be prepared from CO₂.³ In contrast to most liquid hydrogen carriers, reversible storage of H₂ with CO₂ can be achieved using catalytic systems at moderate temperatures and ideally, can be charged and discharged without any chemical input beyond H₂ and CO₂.^{4-6,7}

Homogeneous transition metal complexes supported by pincer ligands can be efficient catalysts for selective CO₂ hydrogenation and HCO₂H dehydrogenation (Fig. 1).^{8,9} The dichotomy between conditions required for CO₂ hydrogenation (favored in basic solution)¹⁰ versus HCO₂H dehydrogenation (favored in acidic solution) presents challenges for a closed-cycle approach.^{4,5} As a result, pH cycling is often required to control storage/release.¹¹ Ruthenium(II) complexes supported by ancillary pincer ligands show the most promise as catalysts for reversible CO₂ hydrogenation/dehydrogenation without

a) Ru(II) H₂ storage catalysts operating without changes in pH/solvent



b) modular catalysts to study structure/activity relationships

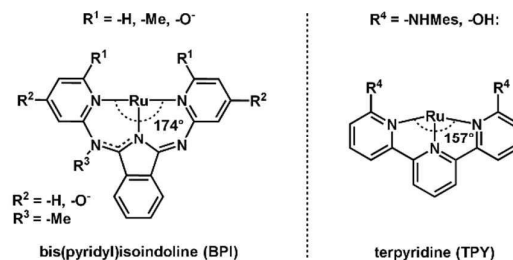


Figure 1. a) Previously reported catalysts for reversible CO₂ hydrogenation without changes in pH or solvent. b) Modular ligand scaffolds for systematic analysis of structure/activity relationships examined in this work.

without adjusting the solvent:base ratio (Fig. 1),⁵ but structural differences between the handful of reported catalysts precludes formulation of general ligand design principles.^{4,12,13} Systematic studies evaluating multiple ligand design parameters using a single ligand platform are needed to provide generalizable design strategies for the development of next-generation catalysts for practical hydrogen storage applications. In this manuscript, we evaluate the CO₂ (de)hydrogenation activity of a series of Ru(II) complexes supported by modular N,N,N-pincer ligands and explore the impact of ligand charge, steric bulk, and bite angle on catalytic activity to establish ligand design guidelines for reversible CO₂ hydrogenation.

^a Department of Chemistry, University of Michigan, 930 N. University, Ann Arbor, MI 48109, USA. E-mail: nszym@umich.edu

[†] Electronic Supplementary Information (ESI) available: synthetic procedures, spectroscopic characterization, and tabulated data. See DOI: 10.1039/x0xx00000x

Bispyridylisoindoline (BPI) and terpyridine (TPY) scaffolds provide substitutional modularity in rigid frameworks, and Ru(II) complexes supported by these ligands catalyze CO₂,¹⁴ carbonyl,^{15,16} and nitrile hydrogenation.¹⁷ Efficient catalysts for reversible CO₂ hydrogenation must present a finely balanced set of properties, including M-H hydricity, M-H₂ pK_a, and dispersive/repulsive effects, which can be impacted by ligand properties such as net charge, bite angle, and steric bulk. We therefore selected a series of Ru(II)-BPI and Ru(II)-TPY complexes that systematically vary these properties through the presence or absence of charged heteroatoms and substituents adjacent to the substrate binding site, and studied the individual impact of these parameters on catalytic activity for both CO₂ hydrogenation and HCO₂H dehydrogenation (**1-9**).

Hydrogenation conditions were optimized with **4** as a catalyst. Solvent (dioxane, DMF, MeCN, 2-MeTHF, toluene, *o*-dichlorobenzene, NEt₃), base (0.4 M K₂CO₃, Cs₂CO₃, KO^tBu, K(N(SiMe₃)₂), KOH, 1,8-diazabicyclo(5.4.0)undec-7-ene (DBU), NEt₃), catalyst loading, temperature, and CO₂/H₂ pressure were systematically screened.[†] This established DBU/DMF as a suitable base/solvent pair, and optimized conditions for hydrogenation were set at 0.4 M DBU, 120 °C, 6:70 atm CO₂:H₂, 18 hours reaction time, and 0.001 mol % catalyst loading in DMF solvent. **4** provided 53% HCO₂⁻ yield with respect to DBU (53,000 TON) under these conditions, and were used for systematic comparison between different catalysts. This base/solvent combination has been previously employed in reversible CO₂ hydrogenation systems.^{13,18}

The conditions for HCO₂H dehydrogenation were selected to simulate the state of a reaction mixture at the end of a complete CO₂ hydrogenation cycle carried out using the optimized conditions noted above (0.4 M HDBU⁺/HCO₂⁻ in DMF, 120 °C) but run at atmospheric pressure in open reactors to permit the escape of CO₂ and H₂. The efficiency of HCO₂H decomposition to CO₂/H₂ was determined using NMR spectroscopy against an internal standard. With **4** (0.005 mol %), these conditions afforded a 10% decrease in HCO₂⁻ concentration in 3 hours, corresponding to 2,100 TON (TOF (h⁻¹): 700).

The impact of ligand charge / donor ability on (de)hydrogenation activity was investigated through comparison of BPI-supported Ru(II) complexes **1-3** (Fig. 2). Each of these complexes contain similar steric environments surrounding Ru(II) with different charges. Complex **1** should be in a fully deprotonated state during hydrogenation and dehydrogenation catalysis due to the presence of a large excess of free DBU (100,000 equiv) and the low pK_a of the pendent -OH groups (~8),¹⁹ providing a trianionic ligand. **2** contains a monoanionic ligand, while methylation of **2** affords the neutral ligand in **3**.[†]

These modulated pincer ligand charges are expected to translate to different hydricity/pK_a values for Ru-H/Ru-H₂ intermediates in catalysis. Laurency and coworkers reported that cationic Ru-phosphine complexes accelerate HCO₂H dehydrogenation, and proposed that coulombic attraction between Ru(II) and anionic H⁻ and HCO₂⁻ was responsible,²⁰

while Muckerman, Ertem,²¹ Himeda²² and Papish²³ each demonstrated that anionic iridium and ruthenium hydride

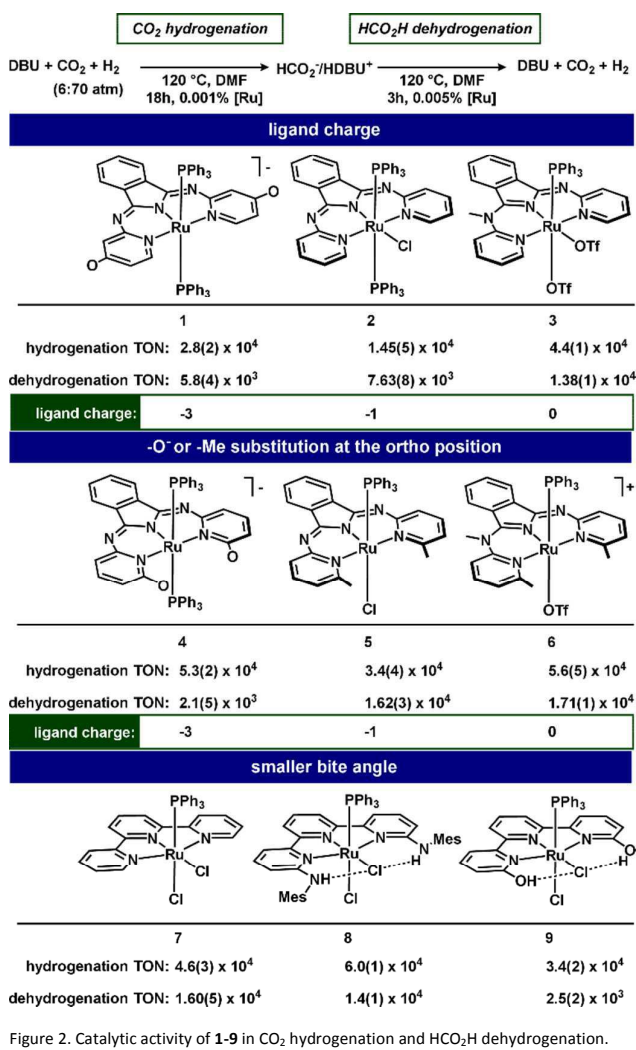


Figure 2. Catalytic activity of **1-9** in CO₂ hydrogenation and HCO₂H dehydrogenation.

complexes exhibit accelerated CO₂ hydrogenation activity, and proposed that enhanced hydricity was responsible. Increasing pincer ligand charge from -3 to 0 afforded increased dehydrogenation activity across the series (TON: 5,800 (**1**), 7,630 (**2**), 13,800 (**3**)). As might be anticipated from previous studies, activity for CO₂ hydrogenation decreased from **1** to **2**. However, **3** was significantly more active than either **1** or **2** (TON: 28,000 (**1**), 14,500 (**2**), 44,000 (**3**)). Together these data suggest that neutral, rather than anionic BPI ligands, improve CO₂ hydrogenation and HCO₂H dehydrogenation activity, which may be a useful ligand design principle for reversible H₂ catalysts.

We previously noted a substrate-dependent effect on hydrogen transfer catalysis by Ru(II)BPI complexes with substituents at the 2- position of the pyridine arms.^{24, 25} We investigated the effect of these substituents on catalytic activity for reversible CO₂ hydrogenation by comparing **1-3** and **4-6**. Catalytic activity for both CO₂ hydrogenation and HCO₂H dehydrogenation increased upon replacement of -H with -Me

or $-O^-$ groups. **6** is one of the most active catalysts capable of mediating reversible CO_2 hydrogenation without changes in pH,^{4, 7, 12, 13, 26} and can achieve high TON (118,000) in CO_2 hydrogenation at high dilution (0.9 ppm) (Fig. 3).

Cooperative H_2 activation, in which pendant bases can facilitate deprotonation of bound $M-H_2$ intermediates, have been widely exploited in the design of efficient catalysts for CO_2 hydrogenation.^{9, 27} We previously demonstrated that the $-O^-$ groups in **4** mediate cooperative H_2 activation.¹⁹ We assessed the viability of a cooperative pathway by comparing the relative activities of **1/4** and **2/5**, in which either a $-O^-$ or $-Me$ group is exchanged for a $-H$ group. Both sets of catalysts provided a similar ratio of activity for CO_2 hydrogenation (**1/4**: 0.52; **2/5**: 0.42), suggesting that steric bulk, rather than metal/ligand cooperativity, is the primary factor controlling the relative activity of **1** and **4**.

Terpyridine (TPY) ligands are isoelectronic with neutral BPI derivatives and offer a smaller bite angle (157° vs. 174°).^{24, 28} The TPY bite angle provides a more accessible coordination site in plane with the pincer ligand, which could either facilitate ligand binding to the metal center or enable undesired pathways such as catalyst dimerization.¹⁶ In comparison with **3**, **7** provided similar activity in CO_2 hydrogenation and HCO_2H dehydrogenation, indicating that bite angle has a small impact on catalytic activity. We previously reported that substitution at the pyridyl 2-positions has a significant impact on oxidant free alcohol/carboxylate conversion activity; $-OH$ groups (**9**) reduced activity, while bulky $-NHMe$ s groups (**8**) increased activity.^{27, 28} We found that these substituent effects also translate to CO_2 hydrogenation activity, with **9** exhibiting the lowest (TON: 34,000) and **8** the highest (TON: 60,000) activity for CO_2 hydrogenation in **1-9**.

CO_2 hydrogenation and HCO_2H dehydrogenation reactions typically are influenced by CO_2 or H_2 pressures, consistent with rate-determining H_2 activation or CO_2 elimination. We evaluated the impact of changing CO_2 and H_2 pressure on each of these reactions using **6** as a catalyst. During HCO_2H dehydrogenation, application of 6 atm H_2 reduced HCO_2H dehydrogenation by 17% (TON: 11,400), while 6 atm CO_2 reduced HCO_2H dehydrogenation by 87% (TON: 1,794). Under CO_2 hydrogenation conditions, the relative impact of CO_2 and H_2 pressure on catalytic efficiency was reversed. Lowering the pressure of CO_2 from 6 to 3 atm increased the yield of HCO_2^- by 22% (TON: 10,240 (3 h, 0.005% **6**)), and lowering the pressure of H_2 from 70 to 35 atm decreased the yield of HCO_2^- by 51% (TON: 4,110 (3h, 0.005% **6**)). The activity of **6** during CO_2 hydrogenation was not appreciably effected by the presence of $\sim 160,000$ equiv. $Hg(0)$, and the effect of altered CO_2 and H_2 pressure was consistent through **4-6**. We hypothesize that less anionic ligand charge improves the efficiency of HCO_2H dehydrogenation and CO_2 hydrogenation due to an increase in Ru electrophilicity. This would be consistent with CO_2 elimination as the rate determining step in HCO_2H dehydrogenation, and H_2 activation as rate determining during CO_2 hydrogenation.

Catalytic HCO_2H dehydrogenation can be used to generate

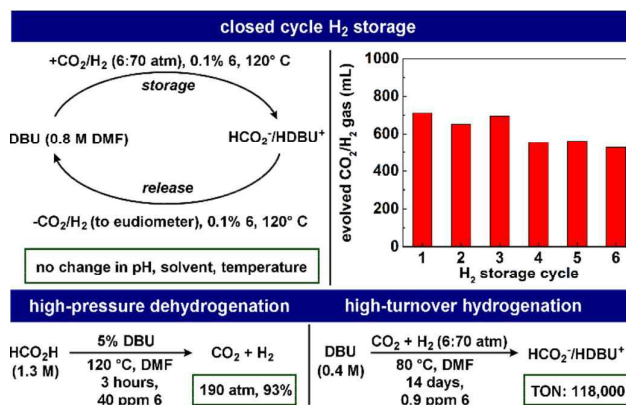


Figure 3. Operation of a closed-cycle H_2 storage device using **6** as a catalyst, high-pressure HCO_2H dehydrogenation, and high-turnover CO_2 hydrogenation.

H_2/CO_2 gas mixtures at high pressures,²⁹ which have applications in fuel cells, H_2/CO_2 gas separations,^{30, 31} and the generation of mechanical power.^{30, 32} We used **6** to generate high pressure H_2/CO_2 gas from HCO_2H in a sealed vessel. Upon heating a 1.3 M DMF solution of HCO_2H containing 5% DBU and 0.004% **6** for 3 hours at $120^\circ C$, the reactor pressure increased to 190 atm.⁵ Venting afforded CO_2/H_2 gas in 94% yield (TON: 247,000, TOF: $82,000\ h^{-1}$), demonstrating that **6** exhibits exceptional activity in the presence of excess HCO_2H .

Finally, we applied the high catalytic activity of **6** to a closed chemical H_2 storage system (no change in pH or solvent). Using 0.1% **6** under standard reaction conditions, CO_2 was hydrogenated to HCO_2H over 30 minutes at $120^\circ C$. The reactor was then cooled, depressurized, and heated at $120^\circ C$ for 30 minutes to release stored H_2/CO_2 gas at ambient pressure with the measured volume indicating a $HCO_2H : DBU$ ratio of at least 1:1.3 before dehydrogenation. $HCO_2H : DBU$ ratios above 1.5 have previously been generated through CO_2 hydrogenation in DMF.¹³ The cycle was repeated six times, with a gradual reduction in evolved H_2/CO_2 to 94% relative to DBU. At the end of the sixth cycle, the evolved gas did not contain detectable quantities of CO (GC/TCD, detection limit: 0.01%).

In conclusion, we have used a series of Ru(II) complexes bearing systematically varied N,N,N- pincer ligands to evaluate the effect of ligand charge and bite angle in reversible CO_2 hydrogenation. Using this approach, we identified increased ligand charge and the presence of *o*-substituents as ligand properties that can increase catalytic activity for both reactions. This algorithm identified an optimized catalyst for closed-cycle reversible storage of H_2 and dehydrogenation of HCO_2H to generate high pressure H_2/CO_2 .

Acknowledgments

This work was supported by the University of Michigan Department of Chemistry, a University of Michigan Energy Institute Summer fellowship (JLC), and an NSF CAREER (grant CHE-1350877). We thank William T. P. Denman, Allen M. Donne, James L. Lawniczak and Michael T. Payne for examining

HCO₂H dehydrogenation in Chemistry 482, an undergraduate laboratory course at UM. X-ray diffractometers were funded by the NSF (CHE 1625543).

Conflicts of interest

There are no conflicts to declare.

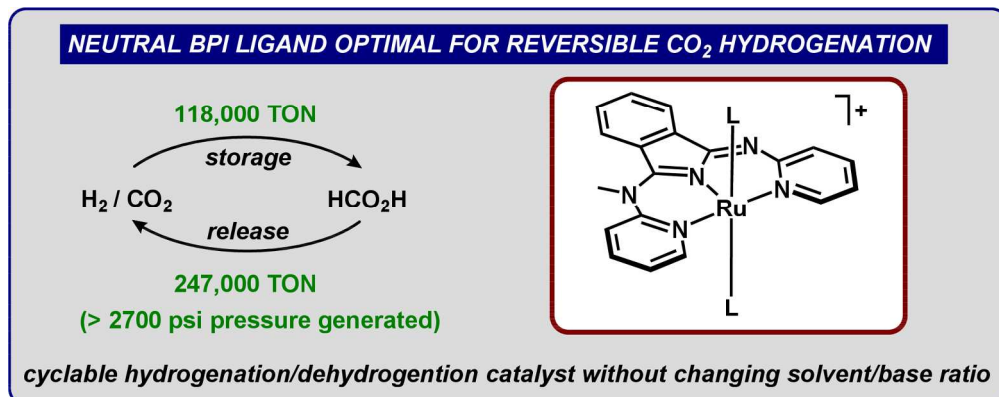
Notes and references

‡ See SI for details. HCO₂⁻ was quantified through ¹H-NMR spectroscopy.

† Note that changes to the overall charge of the BPI ligand may affect Ru hydricity as well as primary coordination environment and ligand exchange reactions.

§: The maximum pressure we could measure was limited by the mechanical strength of our reactor (204 atm)

- X. Zou and Y. Zhang, *Chem. Soc. Rev.*, 2015, **44**, 5148-5180; J. D. Blakemore, R. H. Crabtree and G. W. Brudvig, *Chem. Rev.*, 2015, **115**, 12974-13005; M. G. Walter, E. L. Warren, J. R. McKone, S. W. Boettcher, Q. Mi, E. A. Santori and N. S. Lewis, *Chem. Rev.*, 2010, **110**, 6446-6473; W. Lubitz and W. Tumas, *Chem. Rev.*, 2007, **107**, 3900-3903.
- J. Klankermayer, S. Wesselbaum, K. Beydoun and W. Leitner, *Angew. Chem. Int. Ed.*, 2016, **55**, 7296-7343; E. Gianotti, M. Taillades-Jacquín, J. Rozière and D. J. Jones, *ACS Catalysis*, 2018, **8**, 4660-4680.
- W.-H. Wang, Y. Himeda, J. T. Muckerman, G. F. Manbeck and E. Fujita, *Chem. Rev.*, 2015, **115**, 12936-12973; M. Czaun, J. Kothandaraman, A. Goepfert, B. Yang, S. Greenberg, R. B. May, G. A. Olah and G. K. S. Prakash, *ACS Catalysis*, 2016, **6**, 7475-7484; P. Sponholz, D. Mellmann, H. Junge and M. Beller, *ChemSusChem*, 2013, **6**, 1172-1176; K. Müller, K. Brooks and T. Autrey, *Energy Fuels*, 2017, **31**, 12603-12611.
- S.-F. Hsu, S. Rommel, P. Eversfield, K. Müller, E. Klemm, W. R. Thiel and B. Plietker, *Angew. Chem. Int. Ed.*, 2014, **53**, 7074-7078.
- D. Mellmann, P. Sponholz, H. Junge and M. Beller, *Chem. Soc. Rev.*, 2016, **45**, 3954-3988.
- W.-H. Wang, X. Feng and M. Bao, in *Transformation of Carbon Dioxide to Formic Acid and Methanol*, Springer Singapore, Singapore, 2018, DOI: 10.1007/978-981-10-3250-9_2, pp. 7-42; K. Sordakis, C. Tang, L. K. Vogt, H. Junge, P. J. Dyson, M. Beller and G. Laurenczy, *Chem. Rev.*, 2018, **118**, 372-433.
- W. Leitner, E. Dinjus and F. Gaßner, *J. Organomet. Chem.*, 1994, **475**, 257-266.
- W. H. Bernskoetter and N. Hazari, *Acc. Chem. Res.*, 2017, **50**, 1049-1058.
- Y. Zhang, A. D. MacIntosh, J. L. Wong, E. A. Bielinski, P. G. Williard, B. Q. Mercado, N. Hazari and W. H. Bernskoetter, *Chem. Sci.*, 2015, **6**, 4291-4299.
- R. Tanaka, M. Yamashita and K. Nozaki, *J. Am. Chem. Soc.*, 2009, **131**, 14168-14169.
- J. F. Hull, Y. Himeda, W.-H. Wang, B. Hashiguchi, R. Periana, D. J. Szalda, J. T. Muckerman and E. Fujita, *Nature Chemistry*, 2012, **4**, 383.
- G. Papp, J. Csorba, G. Laurenczy and F. Joó, *Angew. Chem. Int. Ed.*, 2011, **50**, 10433-10435; A. Boddien, F. Gärtner, C. Federsel, P. Sponholz, D. Mellmann, R. Jackstell, H. Junge and M. Beller, *Angew. Chem. Int. Ed.*, 2011, **50**, 6411-6414; J. Kothandaraman, M. Czaun, A. Goepfert, R. Haiges, J.-P. Jones, R. B. May, G. K. S. Prakash and G. A. Olah, *ChemSusChem*, 2015, **8**, 1442-1451.
- G. A. Filonenko, R. van Putten, E. N. Schulpen, E. J. M. Hensen and E. A. Pidko, *ChemCatChem*, 2014, **6**, 1526-1530.
- T. Ono, S. Qu, C. Gimbert-Suriñach, M. A. Johnson, D. J. Marell, J. Benet-Buchholz, C. J. Cramer and A. Llobet, *ACS Catalysis*, 2017, **7**, 5932-5940.
- C. M. Moore and N. K. Szymczak, *Chemical Communications*, 2013, **49**, 400-402; K.-N. T. Tseng, J. W. Kampf and N. K. Szymczak, *Organometallics*, 2013, **32**, 2046-2049.
- C. M. Moore, B. Bark and N. K. Szymczak, *ACS Catalysis*, 2016, **6**, 1981-1990.
- K.-N. T. Tseng, A. M. Rizzi and N. K. Szymczak, *Journal of the American Chemical Society*, 2013, **135**, 16352-16355.
- M. Pschenitzka, S. Meister and B. Rieger, *Chemical Communications*, 2018, **54**, 3323-3326.
- J. B. Geri and N. K. Szymczak, *J. Am. Chem. Soc.*, 2015, **137**, 12808-12814.
- W. Gan, D. J. M. Snelders, P. J. Dyson and G. Laurenczy, *ChemCatChem*, 2013, **5**, 1126-1132.
- M. Z. Ertem, Y. Himeda, E. Fujita and J. T. Muckerman, *ACS Catalysis*, 2016, **6**, 600-609.
- N. Onishi, S. Xu, Y. Manaka, Y. Suna, W.-H. Wang, J. T. Muckerman, E. Fujita and Y. Himeda, *Inorg. Chem.*, 2015, **54**, 5114-5123.
- S. Siek, D. B. Burks, D. L. Gerlach, G. Liang, J. M. Tesh, C. R. Thompson, F. Qu, J. E. Shankwitz, R. M. Vasquez, N. Chambers, G. J. Szulczewski, D. B. Grotjahn, C. E. Webster and E. T. Papish, *Organometallics*, 2017, **36**, 1091-1106.
- K.-N. T. Tseng, J. W. Kampf and N. K. Szymczak, *ACS Catalysis*, 2015, **5**, 5468-5485.
- L. V. A. Hale, T. Malakar, K.-N. T. Tseng, P. M. Zimmerman, A. Paul and N. K. Szymczak, *ACS Catalysis*, 2016, **6**, 4799-4813.
- M. Czaun, A. Goepfert, J. Kothandaraman, R. B. May, R. Haiges, G. K. S. Prakash and G. A. Olah, *ACS Catalysis*, 2014, **4**, 311-320.
- I. Nieto, M. S. Livings, J. B. Sacchi, L. E. Reuther, M. Zeller and E. T. Papish, *Organometallics*, 2011, **30**, 6339-6342; W.-H. Wang, J. T. Muckerman, E. Fujita and Y. Himeda, *ACS Catalysis*, 2013, **3**, 856-860; C. M. Moore, E. W. Dahl and N. K. Szymczak, *Curr. Opin. Chem. Biol.*, 2015, **25**, 9-17; W.-H. Wang, Y. Himeda, J. T. Muckerman and E. Fujita, in *Adv. Inorg. Chem.*, eds. M. Aresta and R. van Eldik, Academic Press, 2014, vol. 66, pp. 189-222; S. Y. de Boer, T. J. Korstanje, S. R. La Rooij, R. Kox, J. N. H. Reek and J. I. van der Vlugt, *Organometallics*, 2017, **36**, 1541-1549.
- S. Sharma, S. K. Singh, M. Chandra and D. S. Pandey, *J. Inorg. Biochem.*, 2005, **99**, 458-466.
- M. Iguchi, H. Zhong, Y. Himeda and H. Kawanami, *Chemistry – A European Journal*, 2017, **23**, 17017-17021.
- M. Iguchi, M. Chatterjee, N. Onishi, Y. Himeda and H. Kawanami, *Sustainable Energy & Fuels*, 2018, DOI: 10.1039/C8SE00087E.
- C. Guan, D.-D. Zhang, Y. Pan, M. Iguchi, M. J. Ajitha, J. Hu, H. Li, C. Yao, M.-H. Huang, S. Min, J. Zheng, Y. Himeda, H. Kawanami and K.-W. Huang, *Inorg. Chem.*, 2017, **56**, 438-445.
- A. N. H., B. J. M. and T. A. M., *Chemistry – A European Journal*, 2017, **23**, 13617-13622.



177x70mm (300 x 300 DPI)